Switching Power Supply Unit For An Autonomous Monitoring System

POSPISILIK MARTIN, ADAMEK MILAN
Department of Security Engineering
Tomas Bata University in Zlin
Nad Stranemi 4511, 760 05 Zlin
CZECH REPUBLIC
pospisilik@fai.utb.cz http://www.fai.utb.cz

Abstract: - There is a project of Autonomous monitoring system being solved at Tomas Bata University in Zlin. Within the framework of this project a small airship driven by ultrasonic detectors is being developed. This airship shall be capable of independent operation in an enclosed hall, bearing a camera or another monitoring system. There are several voltages needed to power the circuits of the airship. To ensure their feeding from a Li-Pol battery, a small and lightweight power supply has been designed. In this article, aspects of designing such power supply unit are analysed. Some attention is also devoted to the wider aspects of using the airships, mainly their advantages of low power consumption, and to the circumstances of employing the developed circuits.

Key-Words: airship, power supply, SMD, accumulator, propeller, monitoring

1 Introduction

Firstly, let us mention a few words about the airships. After their rapid onset at the beginning of the 20th century they seemed to be outdone for a long time, but new technologies have made them suitable for several applications at present. Except of traditional means of travel special unmanned aircrafts were developed after the World War II for several purposes such as for military usage, monitoring of wild animals, aerial photo coverage etc.

The main advantages resulting from employing the airships are:

- low power needed to maintain the machine and its load in the air,
- low noise which makes it excellent for wild animals monitoring,
- low vibration ratio which makes it excellent for aerial photo coverage,
- low flight velocity with the possibility of persisting above the monitored object,
- small area needed to take of or make the landing.

These benefits have been employed in several projects of big airships. For example, let us mention the project AURORA, treating a construction of an airship being capable of move a load of 100 kg to the distance of 100 km, driven by the GPS [8]. Another driving system has been developed at Shanghai University for driving the airships as long as 12 m at the esplanade [10].

Apart from the classical construction of big airships a group of small ones has been developed that cannot operate at the esplanade and their loading capacity is quite low, but they are still sufficient for experiments. Their main physical advantage is a capability of floating in the air with minimal power consumption. With modern Li-Pol accumulators they can stay in the air for several hours bearing several electrical equipment such as monitoring units and so forth. It is obvious that thanks to employing the extracting force of the filling gas there is almost no power needed to hold the machine and its load in the air. In fact it is necessary to balance the load of the airship so it decreased its height slightly when the propellers are off in order it could land in case of any crucial failure of the propellers or the driving system.

According to Dr. Bestaui from University of Evry, France, the general geometrical representation of the airship can be described by Fig. 1 [9]. The axes x, y and z are the principal axes of symmetry, forming a right-handed orthogonal frame. The Cv is a point of centre of volume while Cg is a centre of gravity. Considering the airship as a rigid body, it can rotate around each of the axis. The propeller forces are represented by F which is a force evolved by the main propeller under the angle μ while F_3 is a force evolved by the tail propeller, making the body rotate around the z-axis. The forces created by propellers are needed only to compensate the aerodynamic resistance and/or to change the flight direction. Additionally, some active position

stabilisation may be needed as the persistence of the airship is not negligible.

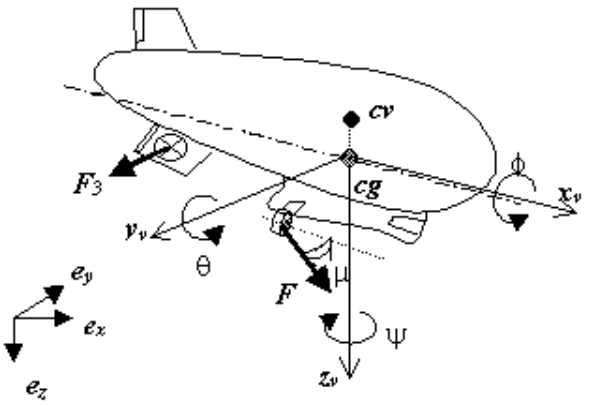

Fig. 1, General geometrical model of the airship according to Dr. Bestaui [9].

The airship operating at the Faculty of Applied Informatics in Zlin is a custom-made modeller product that is capable to bear up to 650 g of load. Equipped with an RC controller, it can be driven like an aeromodel. The bladder is filled with helium and its nominal capacity is 2.7 m^2. The material of the bladder is a special foil made for airships, having a small weight per area unit in order not to decrease the load capability of the airship.

At present, several kits are developed separately in order to create an autonomous monitoring system which is capable of independent operation inside an enclosed hall, being driven by means of ultrasonic detectors and monitoring its neighbourhoods with a web camera. It is supposed that this system will be able to serve other students of the university to treat their own projects on it. All the circuitry must be fed from one Li-Pol accumulator consisting of 2 rechargeable cells with nominal voltage of 3.6 V. In the future, the Li-Pol accumulator might be replaced by a proper supercapacitor in order to increase the operating time while the load capacity stays unchanged. The specific energy of Li-Pol accumulators is around 200 Wh/kg while it is supposed the supercapacitors are going to reach 300 Wh/kg [5].

The orientation of the airship is assured by a set of ultrasonic detectors. A study of employing RFID identificators to determine the accurate position is now processed. The indoor location by RFID technology is described in [6].

2 Initial Demands

In many cases, when thinking about the design of several electrical units, there are not many worries about the power supply and supposing a proper power supply to be connected to our circuit seems to be enough. Unfortunately, the small airship is not included in such group of electrical units. Because the load capacity is limited it is not easy to find satisfactory compromise among the time of operating, percentage of load consumed by bearing the accumulator and the number of electrical units that can be fed, considering their power consumption.

The power consumption of propellers moving the airship can be reduced in two ways. The most significant is the proper controlling the airship

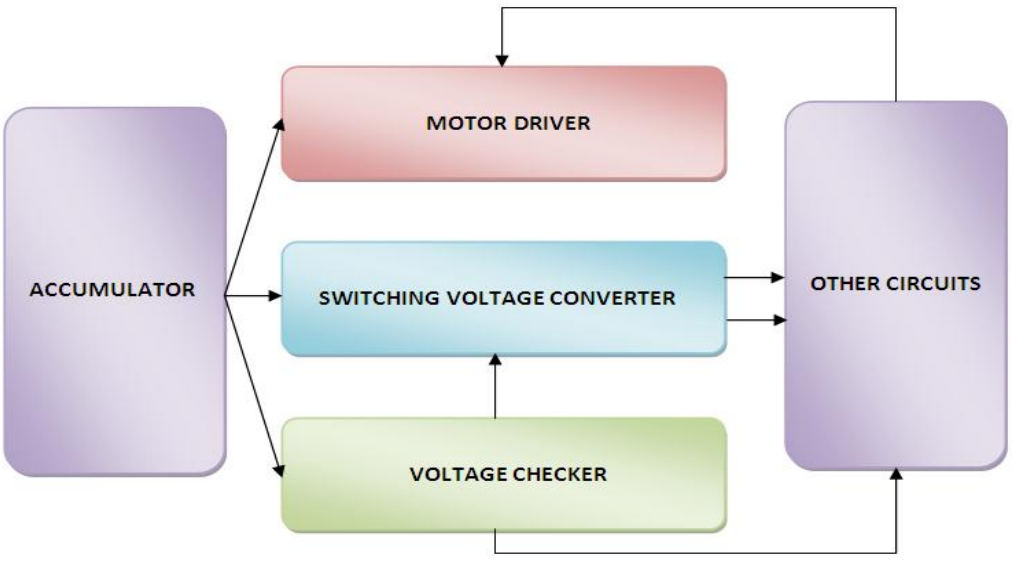

Fig. 2, Block diagram of powering the airship from a Li-Pol accumulator

movement. Several sensors to evaluate the position and flight parameters are needed as well as optimised driving algorithm that does not waste the power of the propellers employing the persistence of the machine. Secondly, wasting the power can be reduced by hardware construction. Because the motors of the propellers can demand relatively high currents, their PWM controller must be connected directly to the accumulator so there were not many components between the accumulator and the motors the resistance of which would lead to losses. In our case, this is taken into account by matching the nominal voltage of propellers and accumulator, which is 7.2 V, and excluding the propeller driver from the power supply module.

The demands on the power supply module have been raised after the all the components to be bore by were chosen. The electrical circuits of the controller employ conventional 5 V microcontrollers so almost the whole circuitry must be supplied with 5 V. One exception has arisen from employing the web camera that was selected for its low weight but needs the supply of 12 V.

The power supply must be lightweight and small. It must be able to protect the accumulator from a deep discharge. It must deliver sufficient current at 5 and 12 V in order to ensure proper feeding of all components and it must not interfere with the components. Considering all these demands including the connection between the accumulator and the propellers a small power supply unit was designed. A block diagram of powering the airship can be seen in Fig. 2.

In order to lower the power dissipation, propeller drivers are connected directly to the accumulator whilst switching voltage converters can be disconnected by means of a safety circuit – voltage checker. The accumulators should not be deeply discharged in order their effective live have not been affected. The voltage checker measures the voltage of each battery cell and is capable of transferring the information about the voltage to the driving unit of

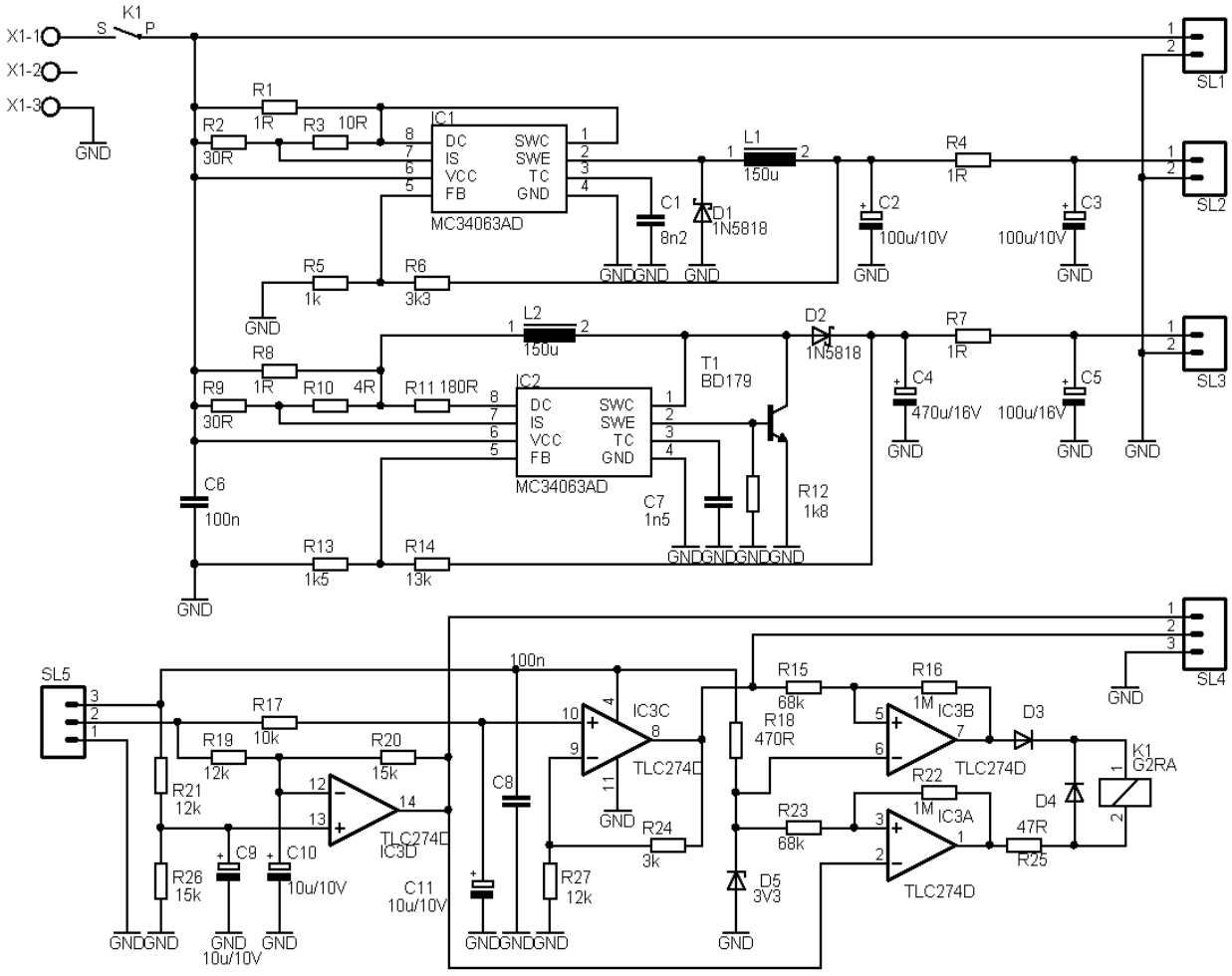

Fig. 3, Power Supply Unit Schematics

the airship. Moreover, if low-battery warning is ignored for any reason, this circuit can disconnect the voltage converters by a relay which causes immediate suspension of the airship's operation. The airship will then slowly decrease its height depending on its weight compensation which is obligatory for the case of any failure occurrence.

3 Power Supply Unit Design

The switching voltage converter is capable of delivering voltages of 5 and 12 V at currents up to 600 mA. Its connection can be seen in Fig. 3.

3.1 Electrical Circuit Description

The power lead from the accumulator is connected to X1 clamps. All the converter circuits can be disconnected by means of a K1 relay. First of all, let us focus to the step-down converter. This converter employs the IC1 custom-designed integrated circuit. It is cheap and easy applicable MC34063 based on a 555 timer platform. It switches the current through L1 coil until a maximum current of 1.25 A is reached. This is set by a voltage drop at R1 resistor. Then the current is switched off and the circuit of the L1 is closed by means of D1 so the current flowing through L1 can fluently lower. After a time period set by a C1 capacitor the cycle repeats. If the voltage at a C2 capacitor exceeds approximately 5.5 V, the converter is blocked and the output voltage decreases for a while. The R4 resistor and C3 capacitor are used instead of a filtering inductor in order to decrease the weight of the unit. The operating frequency is dependent on many factors – the input voltage, L1 inductance and C1 capacitor. Initially it was designed to be around 16 kHz. This is quite low in order to decrease electromagnetic radiation.

The step-up converter also employs MC34063, marked as C2 in the circuit. As high peak currents are needed in order to achieve 12 V at 600 mA at the output, it must have been reinforced with an NPN transistor T1. When switched on, the current through the C2 inductor increases up to approximately 3 A, which is set by the R8 resistor. When this current is reached the T1 is switched off and the current is the pushed through D2 diode to a C4 capacitor. The frequency of this cycle is set by C7 to approximately 16 kHz and the circuit is blocked when the output voltage exceeds 12.5 V. The R7 resistor and C5 capacitor are used instead of a filtering inductor in order to decrease weight.

The third part of the unit is a voltage checker, employing a low-voltage and low-power IC3 operational amplifier TLC274D. This circuit is fed through an SL5 connector to which measuring lead from the accumulator is connected. As the accumulator consists of two cells and these must be checked separately, three conductors are used. The amplifiers IC3D and IC3C are connected as differential amplifiers so they measure voltages of each cell and this voltage is then at their outputs measurable against ground. These voltages can be then conducted to A/D converters of the airship's driving CPU through SL4 connector. In order to employ the full-scale of the A/D converters the voltages are slightly amplified by a factor of 1.25 so if the cells are fully charged at the nominal value of 3.6 V, the output voltages are around 4.5 V. This value can be further scaled by a trimming resistor. The K1 relay is driven by two comparators, IC3A and IC3B and is on when IC3B is in a H level and IC3A is in the L level. The comparators compare the voltage of the reference Zener diode D5 with the voltages at the output of the differential voltage amplifiers. If the voltage of any cell drops under approximately 2.85 V, the relay is turned off and the voltage converters are disconnected. The current through the relay is quite insignificant as it is limited to 18 mA. The stability of the comparators is ensured by setting a 10% hysteresis by means of feedback resistors.

3.2 Integrated Circuits Used

The core of the circuit constitutes of two MC34063 custom-designed integrated circuits to create voltage inductor-based converters that are cheap and quite not complicated, but can achieve interesting results. Its main features are:

- operation at input voltages from 3 to 40 V,
- output current limiting,
- operating frequency up to 100 kHz,
- precision voltage reference,
- switched current up to 1,5 A,
- available packages PDIP-8, SOIC-8 or DFN-8.

The representative block diagram of the circuit can be seen in Fig. 4.

There are three possible configurations of the circuit design, according to the operating mode – step up conversion, step-up conversion or voltage inverter (converting both up and down). The topologies of these modifications are quite common and can be seen in Fig. 5 and Fig. 6.

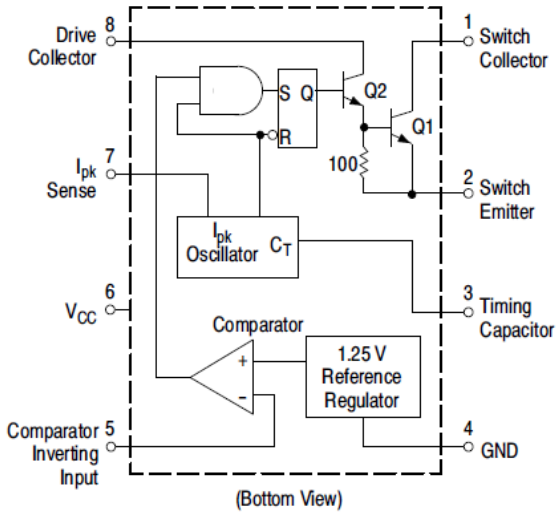

Fig. 4, Representative block diagram of MC34063

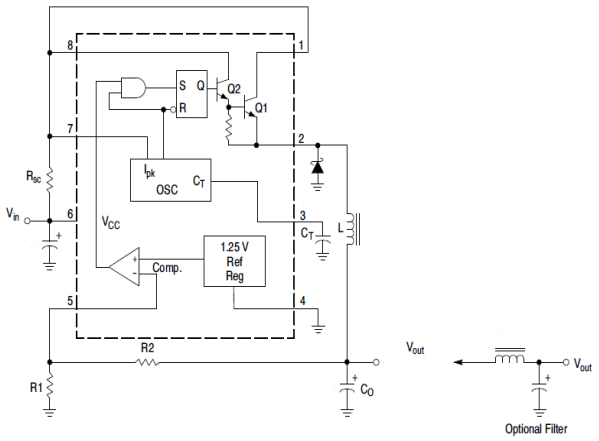

Fig. 5, Typical topology of step-down converter with MC34063

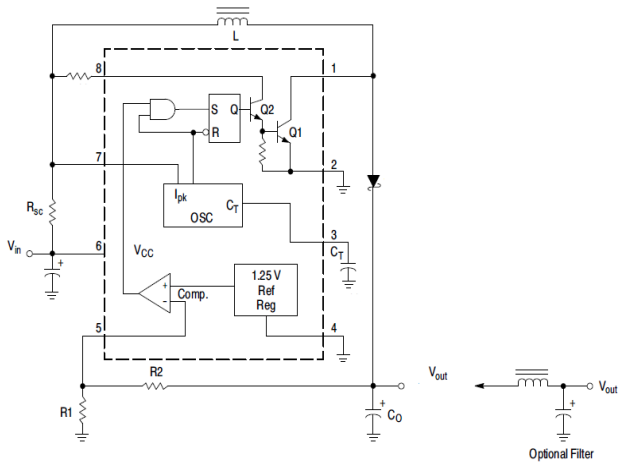

Fig. 6, Typical topology of step-up converter with MC34063

The most significant problem that occurs when employing MC34063 is their asynchronous operation. The converter works until the nominal output voltage is reached and then its oscillator is suspended by the internal reference until the voltage at the output capacitor (it is marked C_O in Fig. 5 and Fig. 6) slightly decreases. The frequency of operation is determined by the input voltage and timing capacitor C_T, but the continuous operation is assured only at the point of maximum output current for which the circuit is designed. At lower output currents the operating frequency is modulated by much lower one resulting from incidental stopping the oscillator at the point of the nominal output voltage overrun. This can cause electromagnetic interferences the pattern of which is quite unknown as both frequencies embody adventitious scattering. As stated below this problem has been struggled by setting the circuits to operate at low frequencies together with optimising the topology of current conductors at the PCB so the electromagnetic radiation was reduced.

Another integrated circuit that has been used at the power supply module is a low-voltage precision quad operating amplifier TLC274D the main advantage of which is that it is capable of operation with voltages from 3 to 16 V and its saturation voltage is as low as 1 V for high output levels and approximately 0.4 V for low level output levels. The output current of each stage is limited at 30 mA which enables direct driving a small relay. This operating amplifier employs a technology called LinCMOS. Except of the capability to operate at low voltages, there are other advantages like high input impedance (> 10^{12} Ω) and low typical input voltage offset (< 1.2 mV). Demands of our application on the parameters are not critical.

3.3 Constructing Step-up and Step-down Converters With MC34063

The MC34063 is a customer-designed integrated circuit intended to be used at low cost and low power switching voltage converters. It is easy applicable and cheap which is why it is predestined for experiments. Designing the converter, the topology of the circuit must be known at first (step-down, step-up, inverting). Selection of proper devices of the circuit is then easy when Tab. 1 is followed.

Tab. 1, Basic design equations [1]

Calculation	Step-Up	Step-Down
t_{on}/t_{off}	$\frac{V_{out} + V_F - V_{in(min)}}{V_{in(min)} - V_{sat}}$	$\frac{V_{out} + V_F}{V_{in(min)} - V_{sat} - V_{out}}$
$(t_{on} + t_{off})$	$\frac{1}{f}$	$\frac{1}{f}$
t_{off}	$\frac{t_{on} + t_{off}}{\frac{t_{on}}{t_{off}} + 1}$	$\frac{t_{on} + t_{off}}{\frac{t_{on}}{t_{off}} + 1}$
t_{on}	$(t_{on} + t_{off}) - t_{off}$	$(t_{on} + t_{off}) - t_{off}$
C_T	$4.0 \times 10^{-5} t_{on}$	$4.0 \times 10^{-5} t_{on}$
$I_{pk(switch)}$	$2I_{out(max)} \left(\frac{t_{on}}{t_{off}} + 1\right)$	$2I_{out(max)}$
R_{sc}	$0.3/I_{pk(switch)}$	$0.3/I_{pk(switch)}$
$L_{(min)}$	$\left(\frac{(V_{in(min)} - V_{sat})}{I_{pk(switch)}}\right) t_{on(max)}$	$\left(\frac{(V_{in(min)} - V_{sat} - V_{out})}{I_{pk(switch)}}\right) t_{on(max)}$
C_O	$9 \frac{I_{out} t_{on}}{V_{ripple(pp)}}$	$\frac{I_{pk(switch)}(t_{on} + t_{off})}{8V_{ripple(pp)}}$

Where:

t_{on}/t_{off} - output pulse ratio [-];
$(t_{on} + t_{off})$ - operating cycle period [s];
t_{off} - interval of being switched off [s];
t_{on} - interval of being switched on [s];
C_T - timing capacity[1] [F];
$I_{pk(switch)}$ - peak switching current[2] [A];
R_{SC} - current-sense resistor value[3] [Ω];
$L_{(min)}$ - minimal inductance[4] [H];
C_O - output filtering capacity[5] [F];
V_{out} - output voltage (designed) [V];
$V_{in(min)}$ - minimal input voltage [V];
V_F - diode forward voltage[6] [V];
V_{sat} - transistors saturation voltage[7] [V];
$I_{out(max)}$ - maximal intended output current [A];
$V_{ripple(pp)}$ - output ripple peak to peak voltage [V];

Notes:
1) Timing capacitors C1 and C7 (setting the operating frequency to approx. 16 kHz).
2) Mentioned in text above.
3) Sensing resistors R1 and R8. In order to reach more suitable values, the voltage is gained through voltage dividers R2/R3 and R19/R20.
4) Inductance of accumulating coils L1 and L2.
5) Output filter is improved with RC members.
6) Voltage drop at fast Schottky diodes D1 and D2.
7) Saturation voltage of internal switching structure or additive output transistor T1, typically less than 1 V.

As obvious from the equations in Tab. 1, the operating frequency varies in dependence on the input voltage. Whilst t_{on} is constant, chosen by the circuit designer, t_{off} varies according to the situation. Practically, it is advisable the capacity of timing capacitor was higher than approximately 400 pF so as there was sufficient allowance for t_{off} to vary according to the input voltage.

3.4 Designing the PCB Considering Aspects of EMC

The most problematic part of the design is the ineligible electromagnetic radiation of the circuit. These problems are partly caused by accidental blocking the circuit operation by the voltage and/or current detection. The chaotic operation caused by current control is described in [7]. Due to the chaotic operation, the electromagnetic spectrum can be very wide so when designing the PCB, several design requirements must have been fulfilled.

The first step to lower the electromagnetic disturbance was setting the operating frequency as low as possible. The second step consists in minimizing that current loops on the PCB which could produce electromagnetic radiation. The third step was using a technique of a ground conductor poured on all free areas of the PCB which ensures partial shielding of the current conductors. Dimensions were restricted in order the whole unit could be mounted into a standardized stannic shielding box.

The PCB is single-layered and most of the devices are SMD type in order not only to decrease dimensions of the unit, but also to shorten the current conductors. The conductors are shaped so they were not right-angled in order to avoid sharp edges on which higher charge density appears. For direct current, longer conductors can be used while the pulse currents are always led by conductors made as short as possible.

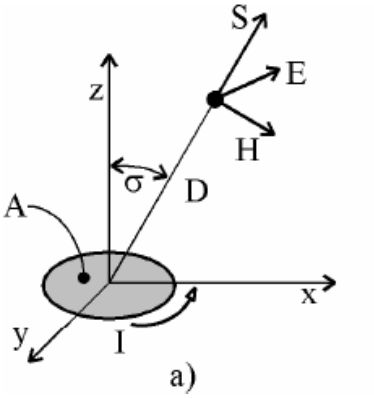

Fig. 7, Electromagnetic radiation by a current loop

Relatively long direct current conductors are blocked by decoupling capacitor C6.

The effect of electromagnetic radiation by a current loop can be seen in Fig. 7. [2]

Let us imagine a loop that carries the current I and lies, in the framework of the orthogonal vector basis, in a horizontal plane (see Fig. 7). The loop area is A. Then S stands for the Poyting's vector which direction represents the direction of the electromagnetic field radiation, while the electric and magnetic components are perpendicular each to other, expressed by vectors E and H. According to [2], the amplitude of both components can be evaluated as follows:

$$|H| = \frac{\pi \cdot I \cdot A}{\lambda^2 \cdot D} \sqrt{1 - \left(\frac{\lambda}{2 \cdot \pi \cdot D}\right)^2 + \left(\frac{\lambda}{2 \cdot \pi \cdot D}\right)^4} \cdot \sin\sigma \quad \left[A \cdot m^{-1}\right] \qquad (1)$$

$$|E| = \frac{Z_0 \cdot \pi \cdot I \cdot A}{\lambda^2 \cdot D} \sqrt{1 + \left(\frac{\lambda}{2 \cdot \pi \cdot D}\right)^2} \cdot \sin\sigma \quad \left[V \cdot m^{-1}\right] \qquad (2)$$

Where:

|H| - intensity of magnetic field [A.m^{-1}],
|E| - intensity of electric field [V.m^{-1}],
I - current flowing by the loop [A],
A - loop area [m^2],
λ - length of the wave [m],
D - distance from the loop in which the proper field is measured [m],
Z_0 - environment wave impedance [Ω],
σ - angle between z and S (see Fig. 7) [°].

The Poyting's vector is a vector product of **H** and **E**.

$$\mathbf{S} = \mathbf{E} \times \mathbf{H} \qquad (3)$$

It is obvious that the radiation decreases with the square of the length of the wave i.e. twice the operating frequency is decreased, the radiation sinks to one quarter. It is also obvious how useful is eliminating the current loop area. When designing the PCB, 0.3 mm isolation distance between the conductors and/or the spilled ground was considered so the area of current loops was eliminated.

The width of the conductors is 0.4 mm which is reasonable for minimising the dimensions according to the dimensions of SMD devices and still suitable for carrying currents up to 1,2 A RMS.

Employing low operating frequencies, conductor capacitances and inductances are negligible as well as parasitic inductive or capacitive coupling.

The layout of the PCB can be seen in Fig. 8. Its dimensions are 70.5 x 51 mm.

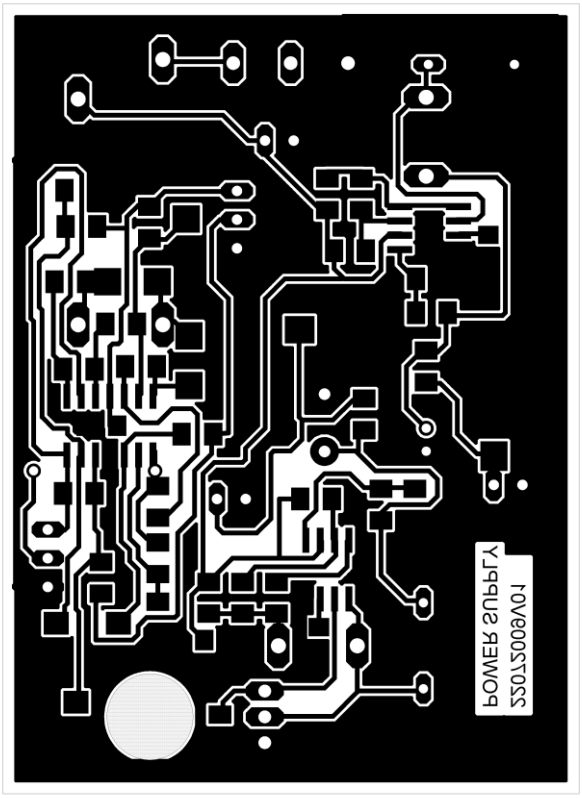

Fig. 8, PCB layout (bottom)

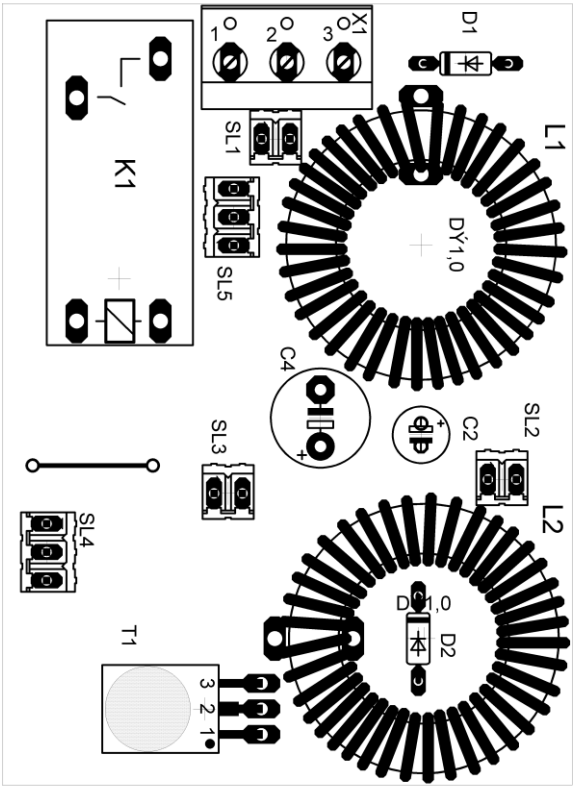

Fig. 9, Top devices displacement

The displacement of the electrical devices can be seen in Fig. 9 for the top side and Fig. 10 for the bottom side (SMD).

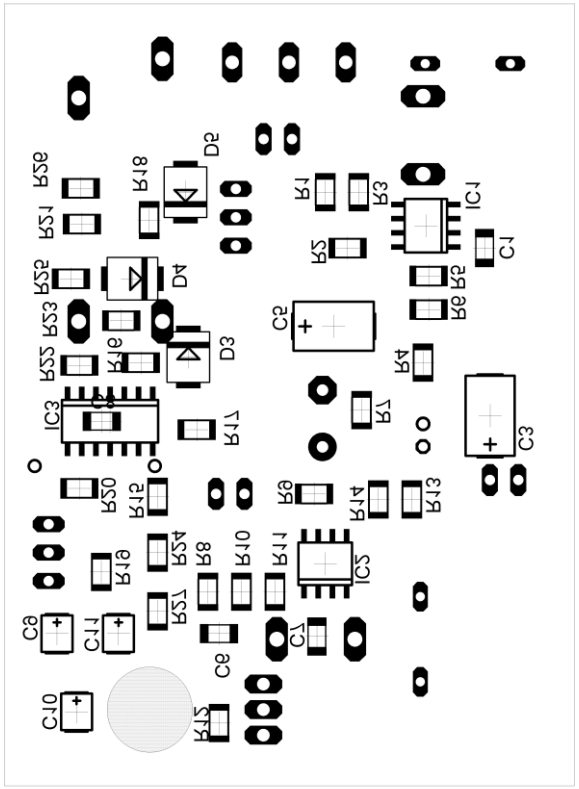

Fig. 10, Bottom (SMD) devices displacement

SMD devices are standard 1208 types, inductors L1 and L2 are toroidal. The transistor T1 is cooled by means of physical contact with the PCB. Capacitors C2 and C4 are to be horizontally oriented so the height of the module was not greater than 25 mm.

3.5 Simulations

Several simulations were processed by Electronics Workbench Multisim 8 application although we do not have the internal model of MC34063 yet. The simulations proved the correctness of basic devices rating.

3.5.1 Step-up Converter at Low Input Voltage and High Output Current

The simulation schema is shown in Fig. 11. The switching transistor BD139 was used instead of BD179 which was not included in the application's database, but the key parameters of the transistor were corrected in order the model respected BD179 parameters (mainly the collector current which is twice as high). The 180 Ω resistor simulates R11 from Fig. 3. The MC34063 was replaced by a clock source operating at 16 kHz with 60% duty cycle. The input voltage was decreased from 7.2 to 6.2 V and the output was loaded with 20 Ω resistor simulating the load. In series with the inductor 0.5 Ω resistor was added to simulate losses in the inductor and the conductors. The diode was neglected because its dynamic behavior influence at such low frequency as 16 kHz is negligible. Its 0.3 V drop is simulated by an additive DC supply (the diode is Schottky type). Under these circumstances the output voltage is 12.0 V with the load current 0.6 A. The ripple is 4.2 mV. The graphs of voltage and current progression can be seen in Fig. 12, 13 and 14.

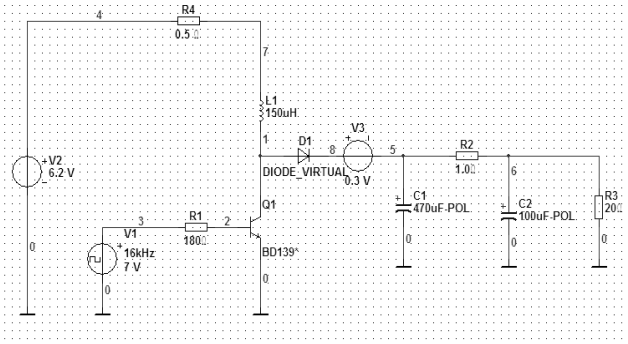

Fig. 11, Step-up converter simulation

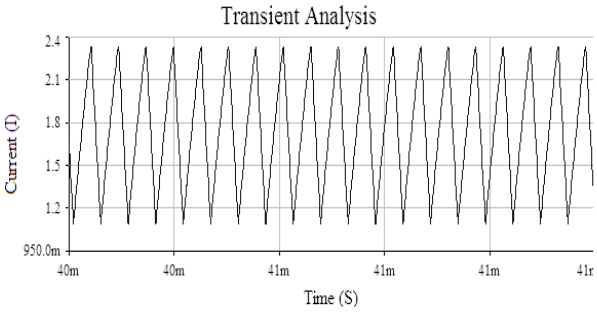

Fig. 12, Inductor current

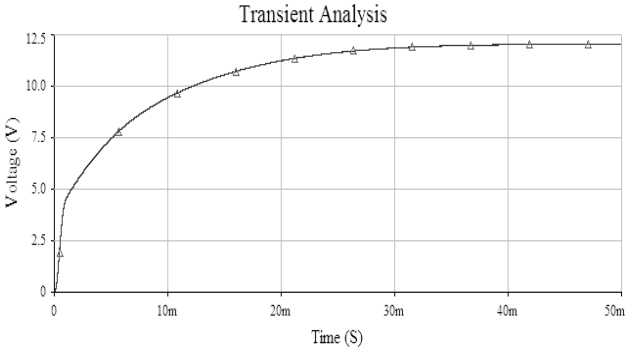

Fig. 13, Output voltage at first 50 ms

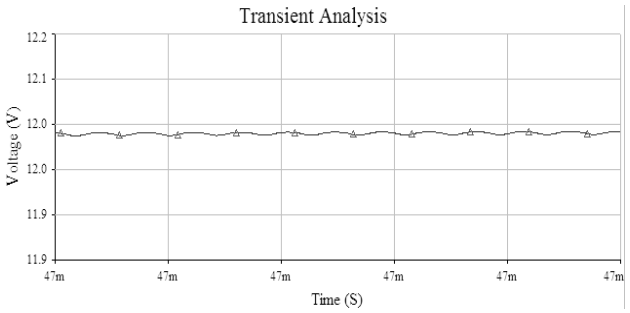

Fig. 14, Output voltage ripple

3.5.2 Step-down Converter at Low Input Voltage and High Output Current

Another extreme situation, output of step-down converter at low input voltage and high output current was simulated according to Fig. 15.

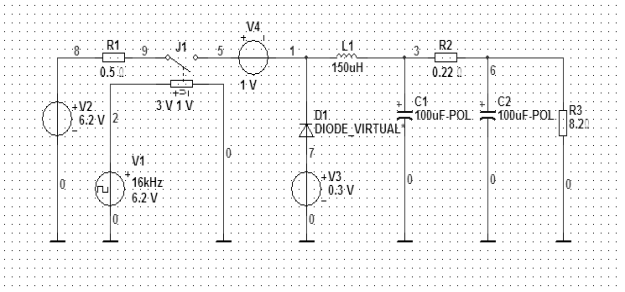

Fig. 15, Step-down converter simulation

In the schematics in Fig. 15, the accumulator with low voltage is represented by a DC voltage source V2. The integrated circuit MC34063 has been replaced by a voltage-controlled switch a voltage source V4 that simulates voltage drop in the internal transistor. The switch is driven by a clock source running at 16 kHz with the duty cycle of 97.5 %. The diode is an ideal one with another voltage source connected in series in order to simulate the junction voltage. The filter resistor (R2 in Fig. 15 and R4 in Fig. 3) was decreased to 0.22 Ω because the previously suggested value of 1 Ω suffered from a high voltage drop. The resistance of input conductors is simulated by 0.5 Ω resistor connected in series with the accumulator.

Under these circumstances the output voltage is around 4.7 V when the output is loaded with 8.2 Ω resistor, which simulates the load drawing approximately 590 mA. The output voltage ripple and the current flowing via the inductor can be seen in Fig. 16 (voltage ripple) and Fig. 17 (current via inductor).

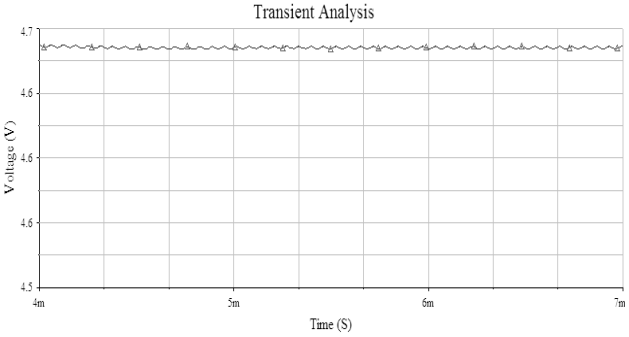

Fig. 16, Output voltage ripple

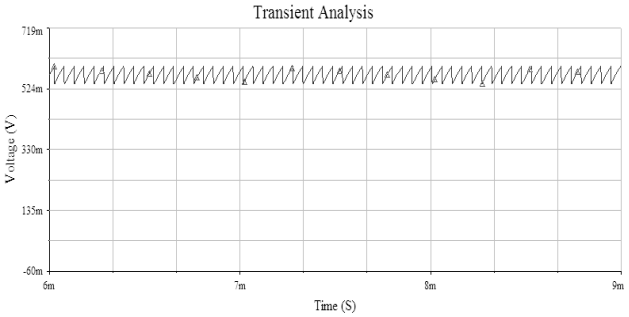

Fig. 17, Inductor current simulation

3.5.3 Voltage checker simulation

In order to verify the design of differential amplifiers at the circuit checking voltage of each cell separately, schema displayed in Fig. 18 was simulated using accurate models of the operating amplifier.

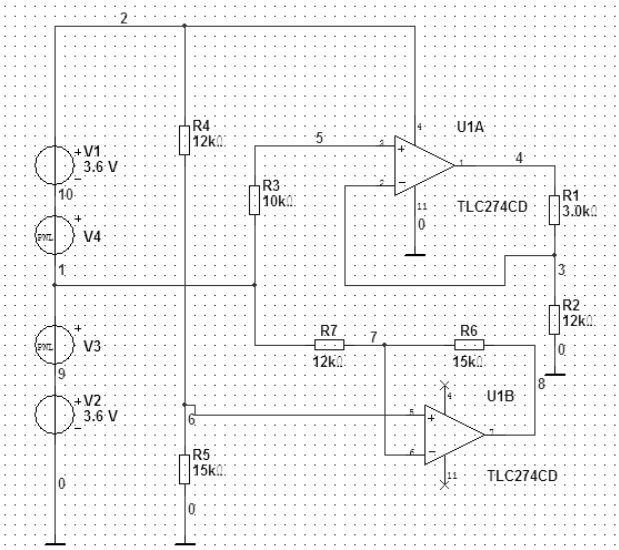

Fig. 18, Simulation schematics of differential amplifiers from voltage checker

In the Fig. 18, the accumulator cells are represented by two DC voltage sources, V1 and V2, that have a nominal voltage of 3.6 V. In addition, two other programmable voltage sources are connected in series with these cells in order to simulate the voltage variations. Firstly, the voltage of V3 falls down by 1 V, than rises up by 2 V and at the end it goes back to 0 V. It simulates the undervoltage and overvoltage of the lower cell. Secondly, the same process is done by V4 while the V3 stays at 0 V. It simulates the undervoltage and overvoltage of the higher cell. In the graph which can be seen in Fig. 19, both output voltages of the operating amplifiers are displayed. It is obvious that the measuring of cell voltages works properly and both amplifiers are independent.

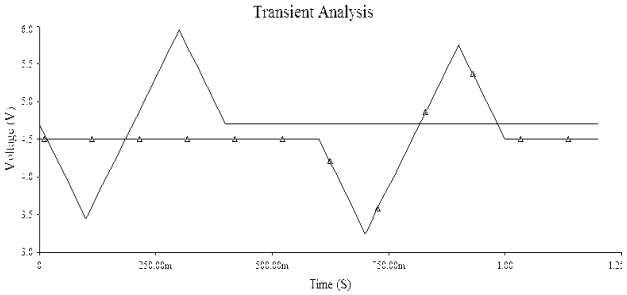

Fig. 18, Output voltage of the differential amplifiers according to the simulation (see text above)

In order to make the graph clear (so both lines could be seen), there was an offset of +0.2 V added to one of the outputs. The nominal output voltage for a cell with a nominal voltage of 3.6 V is 4.5 as stated above.

4 Conclusion

In this article the design of a small and lightweight switching power supply for a small airship operating as an autonomous monitoring system is described as well as some basic aspects of operating small airships inside the buildings. The power supply unit delivers 5 and 12 V to feed the circuits of the autonomous monitoring system described in [3]. It employs easy applicable integrated circuits, considering the demand for low electromagnetic radiation. The parts of the circuit were simulated and the appropriate printed circuit board has been produced. Nowadays the unit is being assembled in order physical tests could be processed.

The project of Autonomous monitoring system is supported by Internal Grant Agency of Tomas Bata University, IGA/45/FAI/10/D.

Acknowledgement

The authors gratefully acknowledge the support of this project from Tomas Bata University in Zlin.

References:

[1]X1. MC34063A, MC33063A, NCV33063A. Datasheet by ON Semi.

[2]X2. Zahlava, V., *Metodika navrhu plosnych spoju*, CVUT Praha, 2000

[3]X3. POSPISILIK, M., ADAMEK, M. 2009. Autonomous Airship. In *Transactions of the VŠB – Technical University of Ostrava, Mechanical Series*, No. 2, 2009, vol. LV, Ostrava, Czech Republic, pp 109 – 114, ISBN 978-80-248-2144-3.

[4]X4. POSPISILIK, M., ADAMEK, M. 2009. Autonomous Monitoring System. In *13th International Research/Expert Conference TMT2009*. Hammamet, Tunisia, pp 777 – 780, ISSN 1840494.

[5] X5. ZHANG, Y., WEI, L., SHEN, X., LIANG, H., Study of Supercapacitor in the Application of Power Electronics, *WSEAS Transactions on Circuits and Systems*, Vol. 8, Issue 6, 2009, pp 508-517, ISSN: 1109-2734

[6] X6. CHEN, R., HUANG, S., A New Method for Indoor Location Base on Radio Frequency Identification, *WSEAS Transactions on Communications*, Vol. 8, Issue 7, 2009, pp 618 – 627, ISSN: 1109-2742

[7]X7. NEGOITESCU, D., LASCU, D., POPESCU, V., CORINA, I., Bifurcation and Chaotic Aspects in Peak Current Controlled Buck-Boost Converters, *WSEAS Transactions on Circuits and Systems*, Vol. 7, Issue 7, 2008, pp 688 – 697, ISSN: 1109-2734

[8] X8. ALBERTO, E. et al, A Semi-Autonomous Robotic Airship for Environmental Monitoring Missions. *Proceedings of the IEEE International Conference on Mechatronics & Automation*. Belgium : [s.n.], 1998. pp 3449 - 3455.

[9] X9. CASTILLO, P., LOZANO, R., DZUL, A., BESTAOUI, Y., *Modelling and Control of Mini-Flying Machines*, Springer, France, 2005, ISBN 1-85233-957-8

[10]X10. JINJUN, R. et al, A Flight Control and Navigation System of a Small Size Unmanned Airship. *Proceedings of the IEEE International Conference on Mechatronics & Automation.* Canada : [s.n.], 2005. s. 1491 - 1496. ISBN 0-7803-9044-X/05/$20.00.